UDC 539.4

Effect of Preliminary Torsional Strain on Low-Cycle Fatigue of Q345B Structural Steel

X. L. Hu,[a] Y. J. Liu,[b,1] C. X. Huang,[b,c] and Q. Y. Wang[a,b,d,2]

[a] Key Laboratory of Underground Science and Engineering, Ministry of Education, College of Architecture & Environment, Sichuan University, Chengdu, China

[b] Failure Mechanics and Engineering Disaster Prevention and Mitigation Key Laboratory of Sichuan Province, College of Architecture & Environment, Sichuan University, Chengdu, China

[c] School of Aeronautics and Astronautics, Sichuan University, Chengdu, China

[d] School of Urban and Rural Construction, Chengdu University, Chengdu, China

[1] liuyongjie@scu.edu.cn

[2] wangqy@scu.edu.cn

Effect of preliminary torsional strain on low-cycle fatigue of Q345B steel was studied. The specimens were first 0, 180, and 360° twisted, then the low-cycle fatigue of Q345B steel was evaluated in the strain range of 0.3–0.8% by the method of axisymmetrical strain. The cycling response, cyclic stress–strain relationship, strain–life relationship, fatigue life prediction model, and seismic stability at different torsion angles were obtained and analyzed. The strain–life curve is shown to slope down as a power function. The fatigue life comes down with preliminary torsional strain at a constant level. The cycling response varied from cyclic hardening to cyclic softening in preliminary torsion, and the cyclic hardening rate increased linearly with the strain amplitude. The parameters of the Coffin–Manson relation are corroborated with experimental data. After heat treatment, the seismic stability of the material is improved, with torsional strain greatly reducing this characteristic. Electron microscope examination of fatigue fracture revealed a fatigue crack initiating on the surface of the specimen. The propagating crack deviated from its direction, and plasticity of the material dropped as a result of preliminary torsional strain.

Keywords: Q345B steel, preliminary torsion, low-cycle fatigue, fatigue life, seismic stability.

Introduction. Q345B structural steel is often used as the main material of critical structures for its high strength, low cost, excellent welding property and toughness. Its stability and toughness play a crucial role in the safety of engineering structures. Q345B steel structures are often subjected to complex alternating loads during service, such as earthquake, wind, dynamic loads caused by the traffic, and so on. Fatigue failure is the main cause of failure in these structures [1], and sudden fatigue fracture may cause heavy losses. Therefore, the study of fatigue behavior of Q345B steel and its structure is a very important part of the engineering field. It is of great significance to ensure the reliability and safety of the engineering structure.

In engineering applications, the steel structural component is usually made by plastic processing, and the bulk material or its surface have preliminary strains due to twisting, bending, stretching, compression or various combination deformation [2]. Moreover, the steel structure will inevitably suffer torsional stresses in use, which may cause plastic deformation. By now, the low-cycle fatigue behavior of structural steels such as high-strength steel [3], Q345B [4], and 45 steel [5] have been studied in detail. However, less attention has been paid to the effect of pre-strain on the fatigue properties of structural steels. The pre-strain may cause the shear stress and the normal stress on the slip surface of the material. The former may increase the dislocation density and strengthen it, while the

latter will cause plastic damage [6]. Miao et al. [7] and Zheng et al. [8] studied the fatigue properties of steels with different carbon content and low-alloy steels after tensile pre-strain, found that the pre-tensile strengthening had a great effect on the fatigue property of carbon steel, and the incomplete plastic deformation and strain hardening caused by tension had an adverse effect on the test results. Wu and Wang et al. [9, 10] studied the effect of pre-torsion strain on fatigue properties of 45 steel, including cyclic stress-strain characteristics, cyclic hardening and softening properties and low-cycle fatigue life, found that fatigue life was reduced after pre-torsion strain and cyclic stress increased with increase of pre-torsion strain. At present, there is no research report on the effect of pre-strain on fatigue behavior of Q345B structural steel.

In this paper, Q345B steel was pre-twisted to different angles and the effects of preliminary torsional strain on low-cycle fatigue and seismic performance of Q345B steel were studied.

1. **Test Material and Specimen**. The commercial hot-rolled Q345B low-alloy steel of thickness of 20 mm was used in this study. Its chemical component (wt.%) is 0.16 C, 0.35 Si, 1.34 Mn, 0.11 S, 0.22 P, and Fe (remain). The material was heat-treated as shown in Fig. 1. The microstructure of the heat treated Q345B steel is depicted in Fig. 2. It can be seen that the material is mainly ferrite (black area), with a low share of pearlite (white area). The main mechanical properties are as follows; the elastic modulus $E = 205$ GPa, yield strength $\sigma_s = 308$ MPa, and tensile strength $\sigma_b = 495$ MPa.

The fatigue specimen was designed according to the standard GB/T 15248-2008 [11] and machined by a CNC machine. The dimensions of the fatigue specimen are shown in Fig. 3. The surface of the specimen was ground and polished with SiC abrasive papers up to a final grade of 1200 and abrasive paste (minimum grain size 7 μm), respectively.

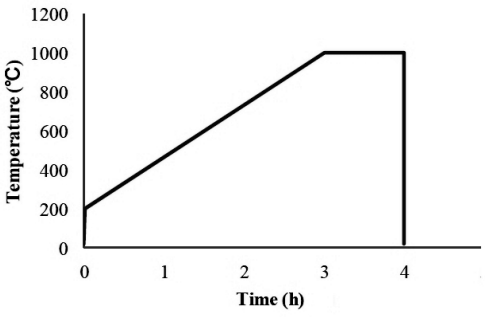

Fig. 1. Heat treatment process.

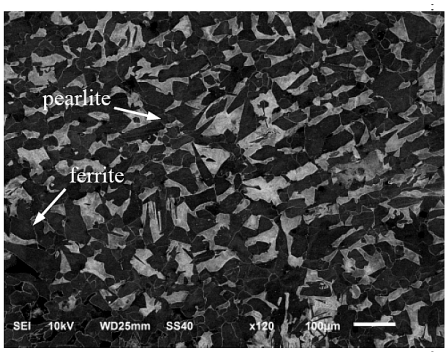

Fig. 2. Microstructure of Q345B steel.

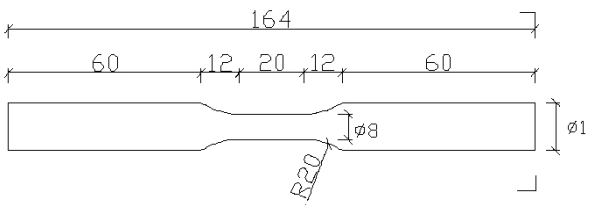

Fig. 3. The dimension of the specimen.

2. **Test Methods**. Torsion tests were carried out via an RNJ-500 type microcomputer-controlled electronic torsion-testing machine.

Tensile tests were conducted using a SHIMADZU AGX-100 universal testing machine. Fatigue tests were carried out by a SHIMADZU EHF-EM200k2-040 fatigue test machine

at room temperature. The strain was controlled by an axial extensometer with a span of 12.5 mm. The loading strain rate was 0.005 s^{-1} , and strain amplitudes were 0.4, 0.5, 0.6, 0.7, and 0.8%. The loading frequency under different strain amplitudes were calculated according to the formula of strain rate expression as follows:

$$\dot{\varepsilon} = \frac{\Delta\varepsilon}{\Delta t} = \left(\frac{\Delta\varepsilon_a}{T/4}\right) = 4 f \Delta\varepsilon_a . \tag{1}$$

3. **Results and Discussion**.

3.1. ***Uniaxial Tensile Test***. Tensile tests were done for specimens with pre-torsion angles of 90, 180, 270, and 360°, respectively, and obtained corresponding mechanical properties are shown in Table 1. It can be seen that with an increase in the pre-torsion angle, the elastic modulus decreased, while the yield strength and tensile strength increased. The tensile curves in the front part are shown in Fig. 4, where the uniaxial tensile behavior of the material is shown to sharply change after pre-torsion, while the yield plateau has disappeared.

Table 1

Mechanical Properties of Q345 Steel

Pre-torsion angle (deg)	E, GPa	σ_s, MPa	σ_b, MPa
0	205	308	495
90	138	358	514
180	128	401	525
360	112	459	576

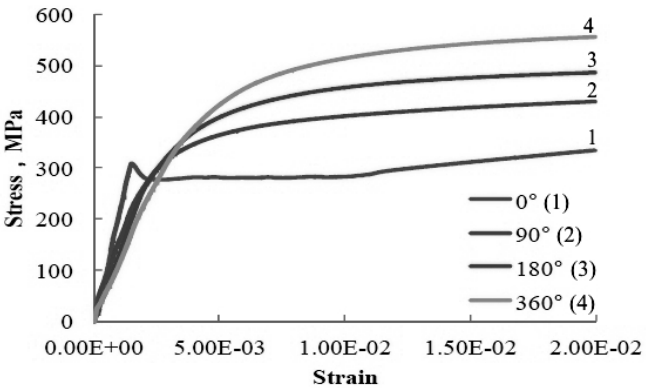

Fig. 4. Uniaxial tensile test.

3.2. ***Cyclic Response Characteristic***. Fatigue tests were carried out on specimens without pre-torsion (0°) and with pre-torsion angels of 180 and 360°, respectively, in the low-cycle range. The cyclic characteristic curves under different strain amplitudes are shown in Fig. 5. It can be seen that the material without pre-torsion firstly had cyclic hardening effect [12], and then entered the stable stress stage until failure. In order to resist the external load, the dislocation arrangement of the material would evolve towards the direction of improving the overall property. Cyclic hardening is mainly caused by the

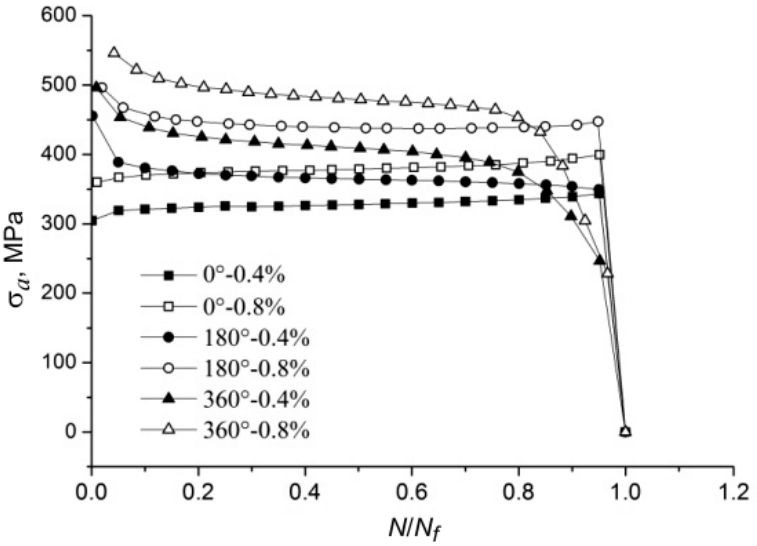

Fig. 5. Cyclic response curves.

dislocation multiplication during cycling [13]. While the material with pre-torsion strain firstly showed cyclic softening. The reason for cyclic softening was that the pre-torsion strain leaded to dislocation rearrangement into a structure with lower density and internal stress [13].

The cyclic hardening rate H can be used to describe the degree of hardening at the initial loading stage, as in [14]:

$$H = \frac{\sigma_{a,sat} - \sigma_{a,1}}{\sigma_{a,1}}, \tag{2}$$

where $\sigma_{a,1}$ and $\sigma_{a,sat}$ are the stress amplitude values in the first and half life cycle. The relation between strain amplitude and cyclic hardening rate are shown in Fig. 6. It implies that the cyclic hardening rate increased linearly with the strain amplitude.

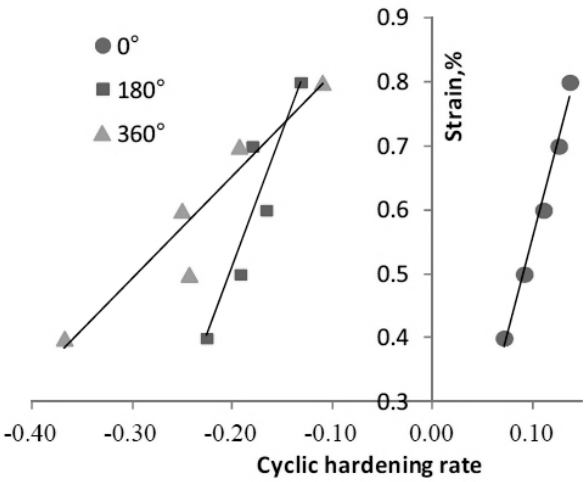

Fig. 6. Cyclic hardening rate.

3.3. ***Strain–Life Curve***. The relationships between strain amplitude and fatigue life were obtained as shown in Fig. 5. Under the same strain amplitude, the fatigue life of the specimen sujected to preliminary torsional load was obviously lower than that of the untreated one, and with an increase in the pre-torsion angle, the related fatigue life decreased. As the cyclic loading amplitude increased, the fatigue life decreased gradually, and the dependence between the strain amplitude and fatigue life was properly described by a power function.

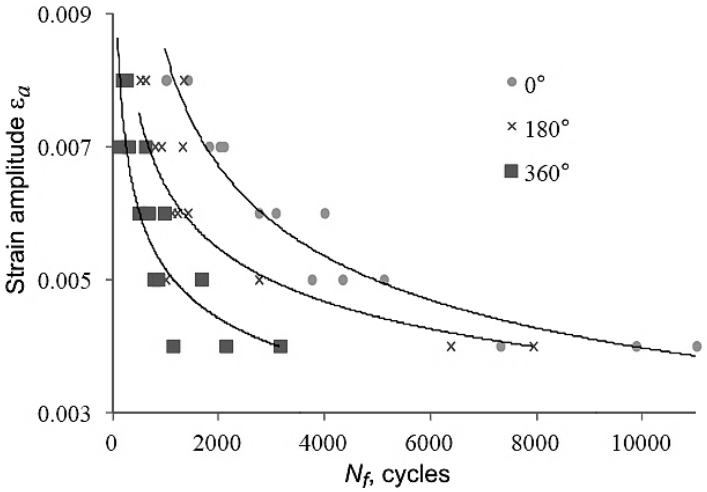

Fig. 7. Strain–life curve.

According to the Coffin–Manson formula [15, 16], the relationship between strain and life was shown as follows:

$$\frac{\Delta\varepsilon_t}{2}=\frac{\Delta\varepsilon_e}{2}+\frac{\Delta\varepsilon_p}{2}=\frac{\sigma'_f}{E}(2N_f)^b+\varepsilon'_f(2N_f)^c, \tag{3}$$

where σ'_f, b, ε'_f, and c are fatigue strength coefficient, fatigue strength index, fatigue plasticity coefficient, and fatigue plasticity index, respectively. The corresponding values could be obtained by fitting the experimental data. The resulting expressions are listed as Eqs.(3)–(5), respectively, and related curves are shown in Fig. 7. The data in the above plot are seen to be evenly distributed on both sides of the fitting curves, showing that the latter curves are in good agreement with the experimental data:

$$\varepsilon_{a0^\circ}=0.0163(2N_f)^{-0.171}+0.3965(2N_f)^{-0.5}, \tag{4}$$

$$\varepsilon_{a180^\circ}=0.0092(2N_f)^{-0.107}+0.1132(2N_f)^{-0.514}, \tag{5}$$

$$\varepsilon_{a360^\circ}=0.0068(2N_f)^{-0.075}+0.0866(2N_f)^{-0.554}. \tag{6}$$

3.4. ***Seismic Performance Analysis***. When buildings are subjected to earthquake loads, most of the energy is absorbed by the steel structures. Therefore, energy consumption of steel directly affects the seismic performance of buildings. Previous studies pointed out that [13], when the seismic load reached about 100 cycles, the building was most likely to

collapse. Assuming that the fatigue life of the material was $N_f = 100$, the greater the cyclic energy absorption rate was, the stronger the energy dissipation capacity of the material. Upon the substituion of $N_f = 100$ into Eqs. (3)–(5), strain values could be obtained as $\varepsilon_{a0°} = 3.46\%$, $\varepsilon_{a180°} = 1.26\%$, and $\varepsilon_{a360°} = 0.92\%$. According to the experimental data, when the cyclic cycle reached 100 cycles, the stress and strain were basically stable. Therefore, the value of σ_a could be obtained according to the ε_a value and then values of $\sigma_a \Delta\varepsilon_t$ were calculated. The energy absorption rate of the heat-treated Q345B steel without pre-torsion was 39.90 J·cm^3, which was higher than those of as-received Q345B (12.89 J·cm^3), showing that it had better anti-seismic performance. The energy absorption rates of the material with pre-torsion angles of 180 and 360° were only 12.04 and 3.53 J·cm^3, which indicated the reduction by 69.8 and 91.2%, respectively, as compared to the untreated one. Therefore, the preliminary torsional strain greatly reduced the seismic performance of the material.

3.5. ***Crack Initiation Life***. In practical engineering, if the initiated crack reached its propagation stage, the material is considered to lose its load-bearing ability. For the material with stable cyclic stress-strain stage, the accumulated damages are characterized by the cyclic stress and strain characteristics. When the material entered the crack propagation stage, the remaining life could be estimated based the relationship between the fatigue crack and the damage evolution [9].

According to the cyclic characteristic curves given in Fig. 5, the point where the stress dropped sharply was considered as the boundary between the fatigue crack initiation and propagation [17]. In this paper, such point was chosen as value at which the constant stress value dropped by 5%. The relationship between the crack initiation life as a percentage of the total life (N_i/N_f) and the strain amplitude are shown in Fig. 8. The variation of the N_i/N_f with the loading strain amplitude exhibited different patterns: it decreased linearly for the untreated material, slightly fluctuated in the range from 80 to 90% for the one subjected to pre-torsion angle of 180°, and increased linearly for the one with pre-torsion angle of 360°.

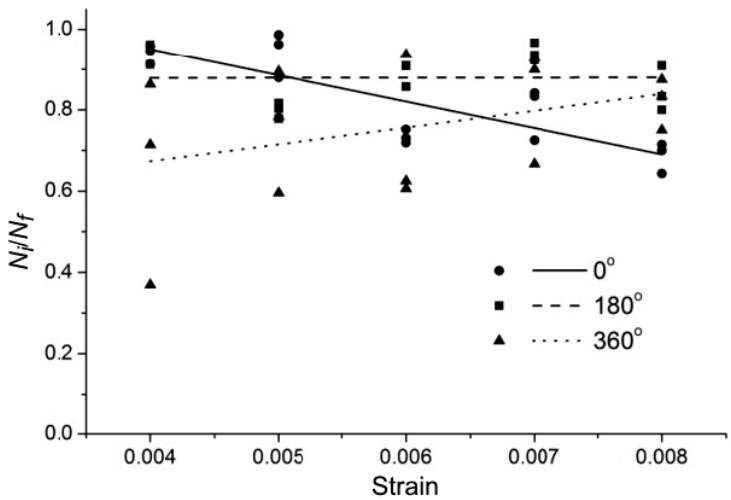

Fig. 8. Cyclic hardening rate.

3.6. ***Fatigue Crack Initiation and Propagation Mechanisms***. The fracture surfaces of broken specimens were investigated by a scanning electron microscope (SEM) as shown in Fig. 9. From the macroscopic features, it could be seen that each fracture surface could be

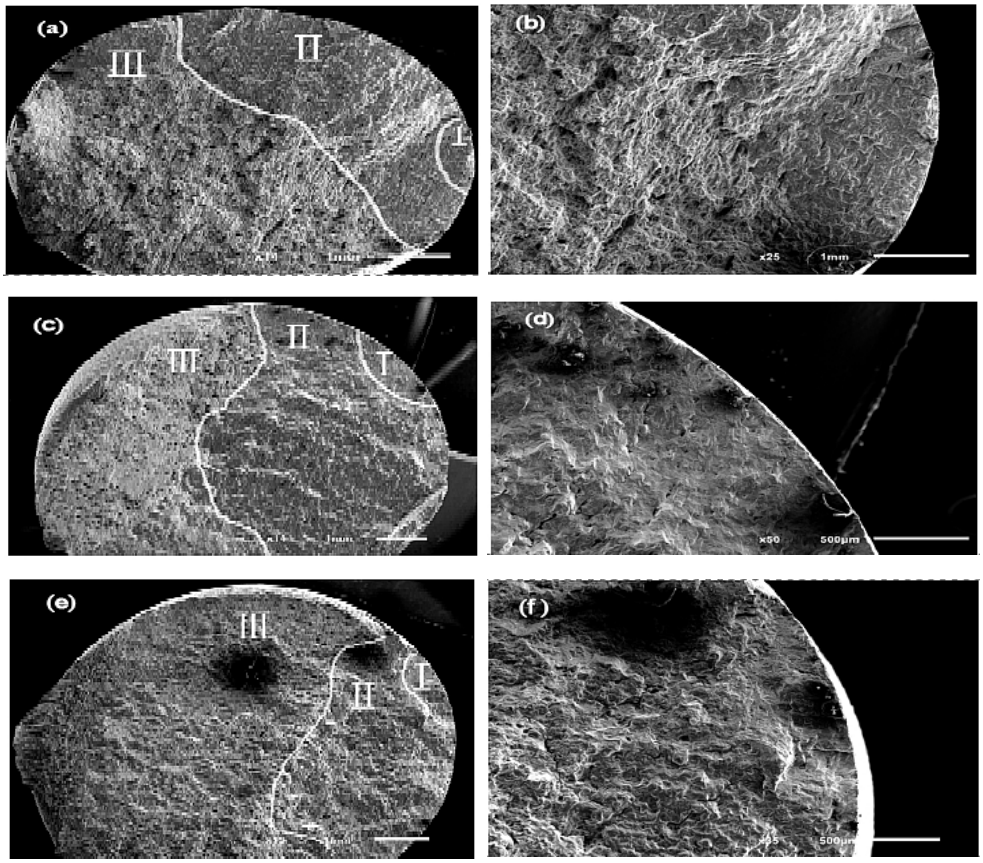

Fig. 9. Fatigue fracture: (a) full view of fracture morphologies (0°); (b) crack initiation area (0°); (c) full view of fracture morphologies (180°); (d) crack initiation area (180°); (e) full view of fracture morphologies (360°); (f) crack initiation area (360°).

divided into three regions: crack initiation area (*I*), propagation area (*II*), and final fracture area (*III*). The fatigue crack originated from the specimen surface and the crack initiation area was bright and smooth. The crack propagation area was relatively smooth, and the part near the final fracture area was rough with secondary cracks and fatigue striations. There were numerous dimples in the final fracture area, indicating a ductile fracture pattern. The cross section of the specimen without pre-torsion was smoother than those with pre-torsions, and the number and height of fatigue striations in the final fracture area increased with the pre-torsion angle. The pre-torsion caused deflection of the fatigue crack propagation direction.

In low-cycle fatigue, fatigue cracks were usually nucleated from the surface of the specimen. With an increase in a cyclic load, many microcracks formed macrocracks by the coalescence and propagation mechanisms. With the propagation of macrocracks, the effective bearing area of the fracture section decreased gradually and the stress increased relatively. When the stress reached the fracture limit of the material, the specimen would fail instantaneously. The number of secondary cracks in the pre-torsion specimens was significantly higher than that in specimens without pre-torsion, and the direction of these secondary cracks was approximately perpendicular to the crack propagation direction. In the final fracture areas of the pre-torsion specimens, the sizes of dimples were relatively smaller and the concave-convex morphologies were larger, which indicated that the pre-torsion reduced the material plasticity.

Conclusions. In this paper, low-cycle fatigue tests of Q345B structural steel specimens subjected to preliminary torsional strain were carried out. The following conclusions can be drawn based on the results obtained.

1. With an increase in the cyclic strain amplitude, the fatigue life decreased gradually, and the strain-life curve decreased via a power function pattern. The fatigue limit of the material is reduced by the preliminary torsional strain.

2. The original material exhibited a cyclic hardening, while specimens subjected to pre-torsion showed a cyclic softening. The cyclic hardening rate increased linearly with the strain amplitude.

3. By calculating the energy absorption rate of Q345B steel, it was concluded that its seismic performance was improved by the heat treatment and strongly reduced by the pre-torsion strain.

4. The variation of the N_i/N_f with the strain amplitude decreased linearly for the material without pre-torsion, remained within the range from 80 to 90% for the pre-torsion angle of 180° one, and increased linearly for the pre-torsion angle of 360°.

5. Fatigue cracks originated from the specimen surface, and the fracture surface could be divided into three regions: crack initiation, crack propagation, and final rupture areas. The pre-torsion caused deflection of the crack propagation direction and reduced the material plasticity.

Acknowledgments. The authors gratefully acknowledge the financial support from the National Science Foundation of China (NSFC-11172188, 11772209), the Program for Changjiang Scholars and Innovative Research Team (IRT14R37), and the International Cooperation Project of Sichuan Provincial Science and Technology Department, China (2016HH0037).

1. S. Nishida, *Failure Analysis in Engineering Applications*, Butterworth-Heinemann (1992).
2. W. Elber, "Fatigue crack closure under cyclic tension," *Eng. Fract. Mech.*, **2**, No. 1, 34–45 (1970).
3. Y. R. Luo, C. X. Huang, R. H. Tian, and Q.Y. Wang, "Effects of strain rate on low cycle fatigue behaviors of high-strength structural steel," *J. Iron Steel Res. Int.*, **20**, No. 7, 50–56 (2013).
4. X. You, Y. J. Liu, M. K. Khan, and Q. Y. Wang, "Low cycle fatigue behaviour and life prediction of Q345B steel and its welded joint," *Mater. Res. Innov.*, **19**, No. S5, 1299–1303 (2015).
5. X. Yang, "Low cycle fatigue and cyclic stress ratcheting failure behavior of carbon steel 45 under uniaxial cyclic loading," *Int. J. Fatigue*, **27**, No. 9, 1124–1132 (2005).
6. J. R. Rice and D. M. Tracey, "On the ductile enlargement of voids in triaxial stress fields," *J. Mech. Phys. Soldis*, **17**, No. 3, 201–217 (1969).
7. D. H. Miao, S. Nishida, and N. Hattori, "Effect of strain aging on fatigue properties of pre-strained carbon steel," *Trans. Jpn. Soc. Mech. Eng. A*, **67**, No. 654, 321–326 (2001).
8. X. L. Zheng, C. Ling, and H. Jiang, "Effects of small prestrain and overloading on the fatigue behavior of high strength low alloy steels," *J. NW Poly. Univ.*, **11**, No. 3, 294–298 (1993).
9. Z. Y. Wu, S. Y. Wang, X. J. Yang, and G. S. Liu, "Effect of torsional prestrain on low cycle fatigue behavior of 35CrMo steel," *J. Exp. Mech.*, **28**, No. 4, 511–516 (2013).
10. S. Y. Wang, M. J. Lin, and J. F. Shao, "Effect of torsional prestrain on low cycle fatigue behavior of steel 45," *J. Mech. Strength*, **20**, No. 4, 300–302 (1998).

11. *GB/T 15248-2008. The Test Method for Axial Loading Constant-Amplitude Low-Cycle Fatigue of Metallic Materials*, Beijing (2008).
12. D. Grenier, S. Das, and M. Hamdoon, "Effect of fatigue strain range on properties of high-strength structural steel," *Mar. Struct.*, **23**, No. 1, 88–102 (2010).
13. G. M. Sheng and S. H. Gong, "The study of cyclic softening and hardening behaviors in a low alloy steel containing vanadium," *J. Chongqing Univ.*, No. 5, 76–85 (1988).
14. D. Ye, S. Matsuoka, N. Nagashima, and N. Suzuki, "The low-cycle fatigue deformation and final fracture behaviour of an austenitic stainless steel," *Mater. Sci. Eng. A*, **415**, Nos. 1–2, 104–117 (2006).
15. L. F. Jr. Coffin, "A study of the effects of cyclic thermal stresses on a ductile metal," *Trans. ASME*, **76**, 931–950 (1954).
16. S. S. Manson, *Behavior of Materials under Conditions of Thermal Stress*, NACA-TR-1170 (1953).
17. G. D. Zhang, H. C. Yu, Y. H. He, and B. Su, "Application research of damage dynamics for low cycle fatigue test," *J. Aerosp. Power*, **22**, No. 9, 1544–1549 (2007).

Received 15. 03. 2018